Unused Housing in Urban China and Its Carbon Emission Impact

ZHENG Hefan[1,*], ZHANG Rongjie[1,*,#], YIN Xinru[1], WU Jing[1,#]

(1. Department of Construction Management, Tsinghua University, Beijing 100084, China; * Z. H. and Z. R. contribute equally to this work; # corresponding authors, Z. R. zhangrj19@mails.tsinghua.edu.cn, W. J. ireswujing@tsinghua.edu.cn)

The intensive utilization of residential space is crucial to the transition to a carbon-neutral residential sector, especially for emerging economies with massive housing construction, such as China, although it has received far less attention in the literature. Here, we develop a novel methodology to estimate the volume of unused housing in urban China, defined as dwelling units that have been built and sold for at least two years but *never* occupied. By early 2021, 17.4% of the housing stock built in China during the first two decades of this century remained unused, with the unused rate being particularly high in most third-tier cities. The construction and operation of unused housing produce 28.26 million tons of CO_2 annually at the national level, which accounts for 4.3% of the Chinese residential sector's carbon emissions, or 19.7% of the carbon emission reductions achieved by China's primary ongoing residential decarbonization efforts from the efficiency perspective. Our projections for 2021–2030 indicate avoiding the further increase of unused housing and utilizing existing unused dwelling units can make a significant decarbonization contribution.

Keywords: unused housing, residential sector, carbon emissions

One-third of worldwide carbon emissions are attributable to the construction and operation of residential buildings[1], making the residential sector a key component of global carbon mitigation. Decarbonizing the residential sector is particularly challenging in emerging economies such as China, where the housing stock continues to rise rapidly. Between 2001 and 2020, China built 11.47 billion sq.m. of urban housing, accounting for about half of the world's new housing[2].

The majority of current efforts to decarbonize the residential sector, in both China and most developed economies, are centered on the "efficiency" perspective, which seeks to reduce the carbon emission intensity associated with the life cycle of residential buildings through measures such as construction material substitution during the materialization stage[3,4] and energy efficiency improvement during the operation stage[5,6]. Nevertheless, the "sufficiency" perspective, which focuses on the intensive usage of residential buildings, plays an even greater role in the pathway to establishing a carbon-neutral residential sector[7-9]. For instance, studies based on the U.S. and several other developed economies imply housing size is the primary determinant of residential carbon emissions in their countries[7,10]. In the context of China, where the volume of newly built housing construction has remained at an increasingly high level during the past two decades, the sufficiency perspective concentrates on the potential oversupply associated with the extensive new construction[11,12]. However, a comprehensive assessment of under-occupied housing and its impact on carbon emissions is absent.

This study focuses on an extreme type of under-occupied housing in urban China, "unused housing," which refers to dwelling units that have *never* been occupied for at

least two years since they were completed and sold to households. Based on a novel approach, our estimate suggests that in early 2021, 17.4% of the housing stock completed between 2001 and 2018 in urban China remained unused. The unused rate is particularly high in cities or housing sectors that are more likely to have experienced a substantial housing oversupply during the last two decades, especially in the majority of third-tier cities. Moreover, our analyses reveal unused housing generates a large volume of carbon emissions and thus remarkably counteracts China's ongoing efforts to decarbonize the residential sector. Taking the year 2020 as an example, the construction and operation of unused housing resulted in the emission of 28.26 million tons of CO_2 at the national level, which accounts for 4.3% of the total residential sector carbon emissions and is equivalent to around 19.7% of the carbon emission reduction achieved by the Chinese government's four major carbon mitigating measures in the residential sector. Naturally, utilizing existing unused housing and avoiding its further expansion should be designated as a top priority in the pathway to establishing a carbon-neutral residential sector in China. Our projections suggest Chinese residential sector's total carbon emissions in 2021–2030 can be reduced by 9.0% if the current unused rate is cut by half by 2030.

Definition and Estimation Method of Unused Housing

Researchers and policymakers typically adopt the term "vacancy" for all unoccupied housing without residents at the time of investigation. Nevertheless, various types of housing vacancy have vastly different implications for decarbonization: some

dwelling units are only temporarily vacant during normal housing turnovers in the market[13,14]; some units are occasionally vacant but still serve households' specific housing demand as seasonal or second homes[15]; and some units have become obsolete due to deteriorating physical or neighborhood conditions[16] but were previously fully inhabited. Whether eliminating the aforementioned types of vacancies without impairing housing market efficiency or resident well-being is feasible remains an open question. Here, we focus on a specific type of vacancy closest to resource waste—dwelling units that remain unoccupied after completion for an extended period of time. For this purpose, we define a dwelling unit as "unused" if (1) it has been sold to a household instead of being held by its developer, (2) it has been completed for at least two years (so that the owner/renter has sufficient time to decorate the interior and move in), and, most importantly, (3) it has *never* been occupied by the time of investigation. From the standpoint of sustainable development, this specific type of housing vacancy should and can be mitigated, if not avoided altogether, and should thus be prioritized when decarbonizing the residential sector. However, no current statistics on the volume or proportion of such unused housing in China (or any other major economy) are available; therefore, we develop our own methodology.

As conceptually illustrated in Fig. 1, the method consists of two core procedures. The first step utilizes the visual information of online-listed dwelling units to identify all unused units in the full-sample online-listed unit observations in the target city, achieving the proportion of unused units among online-listed units (i.e., the listing-based unused rate, or LUR). Typically, the seller or her agent of a listed dwelling unit

in China uploads the listing information onto one or more online platforms for free to disseminate the information to potential buyers[17]. In almost all cases, in addition to the text-format information, the seller or her agent uploads multiple indoor photos of the property to depict the current housing conditions, which has proven crucial for attracting buyers' attention[18,19]. Extended Data Fig. 1 presents representative examples of such indoor photos, based on which we, or a trained deep learning model, can discriminate between unused units (Types I–III in the figure) and units that are currently or were once occupied ("occupied units" hereafter; Types IV and V). As described in detail in "Methods," we develop a supervised deep learning algorithm to classify each photo as unused or occupied, and then aggregate the classification results of all photos associated with each dwelling unit to identify whether the unit is unused. We also use multiple methods to validate the accuracy of the classification results in Supplementary Section 1.

The second step converts the LUR to the stock-based unused rate (SUR, defined as the proportion of unused units throughout the entire housing stock in the target city), which is our main interest, with an emphasis on the correction of two potential sampling biases. First, we adopt the information on the interval between the current listing and the previous transaction of the same unit to correct the potential difference in resale probability between unused and occupied units. Second, we rely on the information from existing literature and macro-level statistics to consider the potential difference in the probability of adopting online listing between unused and occupied units. The details are provided in "Methods."

Insert Fig. 1 about here

Note that, besides the baseline estimate in which we adopt the most likely parameters in these two procedures, we also consider a conservative estimate that tends to achieve the lower bound of SUR.

Results

Volume of unused housing in major cities

We collected information on all dwelling units listed between October 2020 and August 2021 on a leading, anonymous online housing listing platform in mainland China, covering 56 major cities (Supplementary Table 1). In 2020, these 56 cities accounted for 45.0% of the urban population, 53.4% of GDP, and 48.4% of the urban housing completions in China. In each city, we focus on housing communities completed by real estate developers between 2001 and 2018, considering that China's real estate industry only emerged at the beginning of this century.

Fig. 2 depicts the baseline estimate of the city-level SURs during the sample period (we take the mid-point of the sample period, early 2021, to represent the sample period in the following discussions). The corresponding results of the conservative estimate are displayed in Extended Data Fig. 2. We also verify the reliability of the estimates based on other housing market indicators (Supplementary Section 3).

Generally, the results indicate a substantial portion of new homes completed during the first two decades of this century in China had never been occupied by early 2021. Using the city-level aggregated housing completions between 2001 and 2018 as the

weight, the weighted-average SUR of these 56 major cities reached 17.4%; that is, for every six dwelling units completed and sold to households between 2001 and 2018, at least one unit had not been occupied by early 2021. Based on the volume of housing completions in real estate development, the unused rate of 17.4% can be converted to a total of 0.93 billion sq.m. of unused housing in these 56 cities. Two facts may facilitate an intuitive comprehension of this magnitude. First, the unused volume is equivalent to 293% of the annual housing completions in these 56 cities in 2020. Second, the unused volume can accommodate 24.19 million residents, or 6.0% of the urban population in these 56 cities, based on the per capita living space for urban Chinese residents of 38.6 sq.m. in 2020. The conservative estimate puts the unused rate and volume at 12.5% and 0.67 billion sq.m., respectively—a lower but still striking number.

Insert Fig. 2 about here

Fig. 2 also demonstrates substantial inter-city variances, particularly from an across-tier viewpoint. In three first-tier cities—Beijing (3.0%), Shanghai (3.8%), and Shenzhen (4.1%)—the SUR is below 5%. Guangzhou is the only first-tier city with a double-digit SUR (14.8%). The second-tier cities witness larger variations: the SUR is moderate in cities such as Suzhou (7.5%), Hangzhou (8.6%), and Tianjin (9.0%), but remarkable in several other second-tier cities in West China, such as Chengdu (17.4%), Xi'an (24.6%), and Chongqing (25.8%). Most third-tier cities have a large proportion of unused housing, with a weighted-average SUR of 25.3%. Specifically, the unused rate exceeds 30% in nine third-tier cities. Therefore, given that over 250 cities not included in our sample are all third-tier or smaller cities, interpreting the weighted-

average SUR of the 56 sample cities (17.4%) as the lower bound of the national-level SUR is plausible. In this case, the total volume of unused housing at the national level would reach 1.76 billion sq.m. in early 2021—more than half of the overall housing stock in France (2.57 billion sq.m. in 2020).

Fig. 3 presents evidence that such an inter-city variation pattern is consistent with the widespread concern about the potential oversupply in China's housing market. Panel A splits the sample cities into three categories based on the ratio between aggregated housing completions in 2001–2020 and population growth during the same period, which serves as a proxy for excess housing supply in the city. The results indicate the unused rate was significantly higher in cities with a larger supply-demand ratio during these two decades. In the next two panels, we divide the sample cities according to two major housing supply determinants disclosed by the literature. Geographically, Panel B reveals the SUR was significantly higher in cities with higher land supply elasticity, measured by the quantity of flat land area (i.e., area of non-water land with a slope below 15 degrees) in the city, normalized by the population in 2000[20]. Institutionally, Panel C demonstrates the SUR was significantly higher in cities with larger budget deficits in 2001–2020, which serves as a proxy for local governments' dependence on income from residential land sales as off-budget revenues[21]. In other words, a city is more likely to witness a higher SUR if it has more developable land resources for housing development and/or its local authority has to sell more residential land to generate off-budget revenues, which further attests to the linkage between the high unused rate and potential housing oversupply.

Insert Fig. 3 about here

The within-city analysis, as depicted in Fig. 4, also supports such a linkage. Within the same city, the unused housing phenomenon spreads widely across communities, instead of concentrating in a few "ghost towns." As an example, Extended Data Fig. 3 depicts the distribution of community-level unused rates in Xi'an. However, the unused rate is still significantly higher in the suburbs (i.e., communities whose distances to the city center are above the top quartile; Panel A of Fig. 4), which is consistent with the pattern that housing oversupply is more likely to emerge in the suburbs in contemporary China[21]. Similarly, larger dwelling units tend to have a higher unused rate due to potential oversupply (over 140 sq.m. in unit size; Panel B). On the other hand, SUR tends to decrease with building age (Panel C): the unused rate in the building cohort aged between three and five years reached 46.5% and then dropped to 30.0% in the cohort of 6–8 years, 15.8% in the cohort of 9–11 years, and 5.8% in the cohort of 12–20 years. On average, the unused units had remained unused for 6.5 years by early 2021. Nevertheless, we provide the analysis of the "constant-quality" SURs (Supplementary Section 4), which controls for the effect of micro-level housing attributes on the city-level unused rates, and the results demonstrate the patterns shown in Fig. 2 and Fig. 3 are not driven by the composition effect within the cities.

Insert Fig. 4 about here

Effect on carbon emissions

We then convert the estimated volume of unused housing to carbon emissions. As detailed in "Methods," for each square meter of unused housing in early 2021, we

calculate its annually amortized materialization carbon emissions (with an expected service lifespan of 50 years) and annual central heating carbon emissions (only for cities in Northern China), respectively, assuming unused housing does not generate other operating carbon emissions, such as cooking and lighting. We can then calculate the aggregated volume of avoidable carbon emissions associated with all the unused dwelling units in 2020. As listed in Fig. 5, the total volume of preventable carbon emissions associated with unused housing in these 56 cities amounted to 13.32 million tons of CO_2 based on the baseline estimate. Here, we compare the total magnitude with two standards. First, our estimates indicate the total carbon emissions in the residential sector of these 56 cities, including those embedded in construction and materials in new housing and those consumed in operating housing, was approximately 334.56 million tons of CO_2 in 2020; thus, unused housing accounted for 4.0% of the total residential carbon emissions. Second, over the past two decades, the Chinese government has prioritized four key measures for decarbonizing the urban residential sector: lowering carbon intensity in steel and cement production, promoting prefabricated buildings with lower carbon emissions in the construction stage, promoting green buildings with lower carbon emissions in the operation stage, and renovating existing buildings to improve energy efficiency[2,6,9,22-25]. We estimate that, compared with the carbon emissions based on initial intensity factors at the level of the year 2000, these four measures achieved an overall carbon emission reduction of 73.76 million tons of CO_2 in the residential sector of these 56 cities in 2020. In other words, the unnecessary carbon emissions of unused housing were equivalent to 18.1% of the carbon emission reduction by these

four measures. Therefore, China's continuous efforts to decarbonize the residential sector have been significantly impeded by excessive housing supply and the massive volume of unused housing. Unused housing's carbon emissions would have reduced to 10.97 million tons in 2020 if we adopted the conservative estimate (Extended Data Fig. 4), which still accounts for 3.2% of overall residential carbon emissions and offsets 14.7% of carbon emission mitigation in the 56 sample cities.

We also estimate the overall volume of preventable carbon emissions associated with unused housing in the whole country. Specifically, we adopt the weighted-average unused rate of the 56 sample cities (17.4%) as the national-level housing unused rate to take into consideration the other 250 cities. In this case, unused housing cost 28.26 million tons of CO_2 in 2020 based on the baseline estimate. The overall magnitude accounted for 4.3% of the total residential carbon emissions and offset 19.7% of carbon emission mitigation at the national level. In Supplementary Section 5, we also provide another two methods to estimate the unused housing carbon emissions in 2020. The results are close to the current method, although the alternative methods must rely on more assumptions.

Insert Fig. 5 about here

Consistent with Fig. 2, the results in Fig. 5 emphasize the importance of unused housing in third-tier cities. Taking Xi'an, the capital city of Shaanxi Province, with an estimated SUR of 24.5%, as an example, the carbon emissions generated by the construction and operation of unused housing amounted to 0.78 million tons, which accounted for 10.6% of its residential carbon emissions (7.38 million tons) in 2020. By

contrast, in superstar cities with low unused rates, such as Beijing, the impact of unused housing on carbon emissions is modest. Meanwhile, unused housing's carbon emissions are generally higher in Northern China due to the existence of central-heating emissions, which further exaggerate the waste associated with unused housing.

The above findings point out new policy priorities in China's subsequent efforts to establish a carbon-neutral residential sector. On the one hand, policymakers should aim to avoid further housing oversupply, primarily through guiding the residential industry by implementing long-term and annual housing development plans, as well as associated residential land supply schemes, based on high-quality housing demand forecasts. Lowering local governments' reliance on land sales revenues and the resulting residential land oversupply through a reform of the current local fiscal system can also contribute to this goal. On the other hand, local governments can also commit to utilize at least a portion of the unused dwelling units to meet new housing demand, hence partially replacing the demand for new housing construction. This objective can be facilitated by, for instance, imposing a property tax on vacant units, which can increase the homeownership cost for unused dwelling units while minimizing the potential unintended effect on housing demand. Fig. 6 presents our forecast on the impact of these initiatives on China's national-level residential sector carbon emissions between 2021 and 2030. For the benchmark, we assume the Chinese government makes no attempts to eliminate the increase in unused housing or utilize existing unused housing, and hence, the unused rate at the end of 2030 remains at the same level as the end of 2020. Compared with this benchmark scenario, the total carbon emissions in the

residential sector can be reduced by 4.7% if the unused rate can be gradually lowered to 13.0% in 2030 (i.e., 75% of 17.4%), 9.0% if the unused rate can be lowered to 8.7% (i.e., cut by half) in 2030, or 13.0% if the unused rate can reach 4.3% (i.e., 25% of 17.4%) in 2030. Not surprisingly, the potential achievement of unused-housing-related decarbonization measures is particularly pronounced in cities with high unused rates at present, such as Xi'an. We estimate its residential carbon emissions in 2021–2030 can be reduced by 12.7% if its unused rate can be cut by nearly half from 24.6% at the end of 2020 to 12.4% in 2030. By contrast, because the unused rate is currently only 3.0% in Beijing, the potential to further lower its unused rate, as well as its carbon-emission-reduction contribution, is limited. Note that, besides the aforementioned measures in cutting the unused rates, policymakers can also seek to reduce the carbon emissions associated with unused units. In particular, in the northern cities, both technique and policy measures can be implemented to reduce the central-heating emissions of the unused units.

Insert Fig. 6 about here

Conclusion

This study echoes recent literature that highlights the importance of the sufficiency perspective in decarbonizing the residential sector. Using a novel method based on indoor photos of online listings, our calculations in 56 major Chinese cities indicate 17.4% of dwelling units completed between 2001 and 2018 had never been occupied by early 2021, with the phenomenon being most pronounced in relatively smaller cities

that have arguably experienced a massive housing oversupply over the past two decades. The construction and operation of this vast amount of unused housing produce 4.3% of Chinese residential sector's carbon emissions, which could and should be avoided. The avoidable emissions associated with unused housing significantly offset China's ongoing efforts to mitigate the residential sector's carbon emissions. Nevertheless, the research findings also indicate substantial potential for decarbonizing China's residential sector—our forecast implies the total carbon emissions can be reduced by 9.0% in 2021–2030 if the Chinese government can manage to eliminate the current unused rate by half by 2030. Note the vast amount of unused housing is not necessarily a unique phenomenon in China. We encourage researchers and policymakers from other economies, especially developing economies with massive new home constructions, to take unused housing into consideration when designing decarbonization strategies.

References

1. Hamilton, I. et al. *2020 global status report for buildings and construction* (UNEP, 2020); https://globalabc.org/index.php/resources/publications/2021-global-status-report-buildings-and-construction
2. Li, B., Han, S., Wang, Y., Li, J. & Wang, Y. Feasibility assessment of the carbon emissions peak in China's construction industry: Factor decomposition and peak forecast. *Sci. Total Environ.* **706**, 135716 (2020).
3. Mishra, A. et al. Land use change and carbon emissions of a transformation to timber cities. *Nat. Commun.* **13**, 1-12 (2022).
4. Heeren, N. et al. Environmental Impact of Buildings What Matters? *Environ. Sci. Technol.* **49**, 9832-9841 (2015).
5. Leibowicz, B. D. et al. Optimal decarbonization pathways for urban residential building energy services. *Appl. Energy* **230**, 1311-1325 (2018).
6. You, K., Ren, H., Cai, W., Huang, R. & Li, Y. Modeling carbon emission trend in China's building sector to year 2060. *Resour. Conserv. Recycl.* **188**, 106679 (2023).
7. Berrill, P., Wilson, E. J., Reyna, J. L., Fontanini, A. D. & Hertwich, E. G. Decarbonization pathways for the residential sector in the United States. *Nat. Clim. Chang.* **12**, 712-718

(2022).
8. Zhong, X. et al. Global greenhouse gas emissions from residential and commercial building materials and mitigation strategies to 2060. *Nat. Commun.* **12**, 1-10 (2021).
9. Zhu, C., Li, X., Zhu, W. & Gong, W. Embodied carbon emissions and mitigation potential in China's building sector: An outlook to 2060. *Energy Policy* **170**, 113222 (2022).
10. Ellsworth-Krebs, K. Implications of declining household sizes and expectations of home comfort for domestic energy demand. *Nat. Energy* **5**, 20-25 (2020).
11. Wu, J., Gyourko, J. & Deng, Y. Evaluating the risk of Chinese housing markets: What we know and what we need to know. *China Econ. Rev.* **39**, 91-114 (2016).
12. Jin, X. et al. Evaluating cities' vitality and identifying ghost cities in China with emerging geographical data. *Cities* **63**, 98-109 (2017).
13. Rosen, K. T. & Smith, L. B. The price-adjustment process for rental housing and the natural vacancy rate. *Am. Econ. Rev.* **73**, 779-786 (1983).
14. Horn, K. & Merante, M. Is home sharing driving up rents? Evidence from Airbnb in Boston. *J. Hous. Econ.* **38**, 14-24 (2017).
15. Gallent, N., Mace, A. & Tewdwr-Jones, M. *Second homes: European perspectives and UK policies*. (Routledge, 2017).
16. Cohen, J. R. Abandoned housing: Exploring lessons from Baltimore. *Hous. Policy Debate* **12**, 415-448 (2001).
17. Wang, X., Li, K. & Wu, J. House price index based on online listing information: The case of China. *J. Hous. Econ.* **50**, 101715 (2020).
18. Benefield, J. D., Cain, C. L. & Johnson, K. H. On the relationship between property price, time-on-market, and photo depictions in a multiple listing service. *J. Real Estate Financ. Econ.* **43**, 401-422 (2011).
19. Luchtenberg, K. F., Seiler, M. J. & Sun, H. Listing agent signals: Does a picture paint a thousand words? *J. Real Estate Financ. Econ.* **59**, 617-648 (2019).
20. Saiz, A. The Geographic Determinants of Housing Supply. *Q. J. Econ.* **125**, 1253-1296 (2010).
21. Gyourko, J., Shen, Y., Wu, J. & Zhang, R. Land finance in China: Analysis and review. *China Econ. Rev.* **76**, 101868 (2022).
22. Gao, T. et al. Evolution and projection of CO2 emissions for China's cement industry from 1980 to 2020. *Renew. Sust. Energ. Rev.* **74**, 522-537 (2017).
23. Chen, W., Yin, X. & Ma, D. A bottom-up analysis of China's iron and steel industrial energy consumption and CO2 emissions. *Appl. Energy* **136**, 1174-1183 (2014).
24. Shen, J., Zhang, Q., Xu, L., Tian, S. & Wang, P. Future CO2 emission trends and radical decarbonization path of iron and steel industry in China. *J. Clean Prod.* **326**, 129354 (2021).
25. Wang, K., Wang, C., Lu, X. & Chen, J. Scenario analysis on CO2 emissions reduction potential in China's iron and steel industry. *Energy Policy* **35**, 2320-2335 (2007).

Methods

Data. The raw data are collected from one of the leading online housing listing platforms in China. Note that although the literature points out that agents may intentionally release fraudulent listings on online platforms to attract attention[17], this possibility is not a concern for this online platform, because it manually verifies the validity of each listing.

Through web spiders, we collected information on the dwelling units listed on the platform in 56 major cities around China between October 2020 and August 2021. We then cleaned the sample using the following procedures: (1) We only kept units in communities completed between 2001 and 2018, because we only consider dwelling units that have been unused for at least two consecutive years after completion; (2) we only kept units in communities in the major districts/counties in the city as listed in Supplementary Table 1; (3) we dropped outliers as the top and bottom 1% listed units in the number of households in the community and unit size, and the top 1% listed units in the number of floors; and (4) for each city, we also dropped the top and bottom 1% listed units in the unit price. Finally, the working sample includes 1,196,585 listings.

For each unit, we collected all the information provided on the listing webpage (see, e.g., Extended Data Fig. 5), including the listing date and price, locational and physical attributes, text descriptions, and, most importantly, all the indoor photos uploaded. We collected 6,577,579 photos for the working sample, giving us an average of 5.5 photos per listed unit. We also list the number of dwelling units and photos included in each city in Supplementary Table 1.

Identifying Unused Dwelling Units. *Training set construction.* We randomly chose 40,000 units with 233,896 indoor photos from the working sample and hired professional taggers to label whether each image belongs to an unused or occupied unit. For the taggers' reference, we provided example photos of unused and occupied units, as well as descriptions of what can be used as references for unused rooms. Following the guidelines, three taggers labeled each photo. We also examined the photos for which the taggers had divergent opinions.

Extended Data Table 1 reports the tag results for all 233,896 photos, and the ratio between unused and occupied classes is about 1:5. Classifiers trained on such a class-imbalanced dataset tend to be overwhelmed by the larger class and ignore the smaller one[26]. More specifically, in our context, the model is likely to over-classify photos as occupied if we directly adopt the original training sample. To avoid this problem, we randomly selected 38,322 photos from the occupied group to adjust the ratio between the two classes is adjusted to 1[27].

Network Architecture. We use ResNet-50, a deep learning network widely used for image classification[28-30], as our backbone network. Different from convolutional networks such as VGG16, ResNet-50 reformulates the layers as learning residual functions with reference to the layer inputs, instead of learning unreferenced functions, enabling the network to be deeper and achieve higher classification accuracy[31]. The architecture of the network we used is depicted in Extended Data Fig. 6. We convert the classification network into a regression network, whose continuous output is more applicable when we comprehensively consider the outputs of all photos belonging to

the same listed unit. More specifically, we use a one-way fully connected layer with sigmoid as the output layer to replace the original 1,000-way fully connected layer with softmax. In the current setting, our network returns a value ranging from 0 to 1, representing the likelihood that the input photo belongs to an unused unit. The key component of our network is the convolutional kernel (illustrated by "Conv" in Extended Data Fig. 6), which is essentially an n×n weighting matrix that extracts features from the outputs of the last layer. In other words, the sequence of stacked convolutional layers can be regarded as a more intricate and sophisticated feature extractor, which transforms the input RGB image into dozens of features that can be comprehended by subsequent layers. The training process is analogous to using the training sample to teach the network which features should be extracted and the relationships between features and regression results. Besides the original tagged images, we generate random horizontal reflections to modify the RGB channel intensities of the input training images to prevent overfitting issues[32].

Training. To accelerate training, we start with the pre-trained parameters of ResNet50, which was trained using IMAGENET, a dataset containing over 1 million images. Then, we fine-tune the model based on our dataset of tagged photos. We randomly choose 90% of the tagged photos as the training set and the remaining 10% as the testing set. Using a batch size of 96 and a learning rate that initializes at 0.002 and decays by 0.9 per 10 epochs, we train the model with an Adam optimizer for 1,000 epochs.

Because the output result is a continuous possibility, we classify the photo based on a designated threshold. Specifically, if the output result is larger than the designated

threshold, the photo is classified as positive (i.e., unused). Similarly, if the output result is smaller than the designated threshold, the photo is classified as negative (i.e., occupied). To select an optimized threshold, we use F1-Score, a commonly used metric for evaluating the performance of deep learning models[33,34], as the evaluation metric. As listed in eq. (1) and eq. (2), True Positives (*TP*) are examples correctly classified as positives, False Positives (*FP*) refer to negative examples incorrectly classified as positives, True Negatives (*TN*) correspond to negative examples correctly labeled as negative, and False Negatives (*FN*) refer to positive examples incorrectly labeled as negatives. *Precision* reflects the capacity of a classification model to identify only relevant data, whereas *Recall* reflects the ability to identify all relevant cases within a dataset[35]. F1-Score is the harmonic mean of *Precision* and *Recall*, allowing it to assess the model comprehensively:

$$precision = \frac{TP}{TP + FP} \tag{1}$$

$$recall = \frac{TP}{TP + FN} \tag{2}$$

$$F_1 = 2 \times \frac{precision \times recall}{precision + recall}. \tag{3}$$

Extended Data Fig. 7 depicts the three metrics at various thresholds. When the threshold is 0.44, we get the highest F1-Score of 0.897, with a *Precision* of 90.1% and a *Recall* of 89.3%. For simplicity, in the baseline estimate, we directly apply the threshold of 0.5 to distinguish between the unused and occupied classes. Under this threshold, *Precision* is 91.4% and *Recall* is 87.5%.

Single Photo Prediction. We send each of the 6,577,579 photos into the trained model.

The mean value of the predicted likelihood is 0.24, whereas the standard deviation is 0.34. As Panel A of Extended Data Fig. 8 shows, the distribution of prediction concentrates around 0 (i.e., 100% to be occupied) and 1 (i.e., 100% to be unused); specifically, 88% of predicted results are smaller than 0.2 or larger than 0.8. Among all the 6,577,579 photos, 1,284,981 (19.5%) have a prediction value larger than the threshold of 0.5 and hence are classified as unused.

Dwelling Unit Classification. For each of the 1,196,585 listed units, we calculate the average prediction value of all the photos associated with the unit as its unit-level prediction value. The unit-level prediction has a mean value of 0.23 and a standard deviation of 0.31. As Panel B of Extended Data Fig. 8 demonstrates, the unit-level predictions are still centered around 0 and 1, with 89% of units possessing a prediction value smaller than 0.2 or larger than 0.8. Given the threshold of 0.5, 211,498 (17.7%) units are identified as unused, while the other 985,087 are identified as occupied.

Converting Listing-Based Unused Rate to Stock-Based Unused Rate. Suppose S dwelling units exist in the housing stock of city X at time T; ρ percent of the stock is still unused (i.e., the stock-based unused rate, or SUR), and 1-ρ has been occupied. Here, we focus on two potential differences between the unused and occupied groups. First, the selling probability may differ between the unused and occupied groups. We assume the selling probability of occupied units during our sample period is p and that of unused units is qp. Second, the degree to which these two groups rely on online platform listings may also vary. We assume δ of occupied units are listed on our online platform, whereas the corresponding ratio for unused units is $r\delta$. Accordingly, LUR can

be calculated as

$$LUR = \frac{S \times SUR \times qp \times r\delta}{S \times (1-SUR) \times p \times \delta + S \times SUR \times qp \times r\delta}. \quad (4)$$

Then, we can have

$$SUR = \frac{LUR}{LUR - LUR \times q \times r + q \times r}. \quad (5)$$

We estimate q, the ratio between the selling probability of unused and occupied groups, based on the transaction record data from the online listing platform. Specifically, for each listed unit, the online platform reports the date of the prior sale of the unit (i.e., when the current owner of the listed unit purchased the unit from the new home or resale market), allowing us to calculate the holding period of the current owner. We can hence calculate the average lengths of holding periods for the unused and occupied groups, respectively, in each city, and q can be calculated as

$$q = \frac{selling\ probability\ of\ unused\ units}{selling\ probability\ of\ occupied\ units} = \frac{\frac{1}{average\ holding\ period\ length\ of\ unused\ units}}{\frac{1}{average\ holding\ period\ length\ of\ occupied\ units}} = \frac{average\ holding\ period\ length\ of\ occupied\ units}{average\ holding\ period\ length\ of\ unused\ units}. \quad (6)$$

For r, the difference in the likelihood of listed units appearing on the online platform, we assume it equals 1 in the baseline estimate based on the following reasons. First, the China Institute of Real Estate Appraisers and Agents (the Chinese counterpart of the National Association of Realtors) reports that over 85% of housing resale transactions in China are assisted by professional agents, who in almost all cases rely heavily on online platforms to disseminate information. Therefore, one can assume a very high proportion of listings would appear on online platforms, leaving little potential for differences between unused and occupied groups. Second, existing studies in both the U.S. and China indicate occupancy status is not a key determinant of whether sellers choose an agent service or online listing service[36,37]. Third, to test whether the

online platform contains significant sampling biases, we collected listing data for five sample cities between November 2020 and March 2021 from both our online platform and another leading online listing platform in China, and then applied the same classification procedures to calculate the city-level LURs for each platform. As Extended Data Table 2 shows, the LURs based on these two platforms are highly consistent; in particular, the LURs for our platform are neither systematically higher nor lower than those based on the other platform. We can thus safely assume the online platform we choose neither oversamples nor undersamples unused units across all online listings.

In the calculation, because Fig. 4 indicates LUR substantially varies with building age, we split the housing communities in a city into four groups according to the year of construction completion. The first three groups include housing communities completed in 2016–2018 (i.e., with buildings aged between 3 and 5 years), 2013–2015 (6–8 years), and 2010–2012 (9–11 years), respectively, whereas the last group comprises communities completed in 2001–2009 (12–20 years). For each city, we first calculate the LUR and q for each building-age cohort. Then, we calculate the SUR for each building-age cohort based on eq. (5). Finally, we calculate the weighted average of SUR for all four building-age cohorts, weighted by the volume of housing completions in the corresponding years in the city as reported by the local statistical authority.

Conservative estimate of the unused rate. We expect the baseline estimate based on the aforementioned parameters to achieve an estimate of the most probable SUR. We

also evaluate a conservative estimate, which we expect to yield a lower bound of SUR. Compared with the baseline estimate, the conservative estimate alters two key parameters. First, in classifying the unused and occupied units based on indoor photos, instead of adopting the conventional threshold of 0.5, we use F0.5-Score as the new metric to get the threshold, which values *Precision* more than *Recall*. F0.5-Score is calculated as follows:

$$F_{0.5} = (1 + 0.5^2) \times \frac{precision \times recall}{0.5^2 \times precision + recall}. \quad (7)$$

We obtain the maximum F0.5-Score of 0.922 when the threshold is 0.7, with *Precision* improving from 91.4% to 95.6% and *Recall* decreasing from 87.5% to 80.7%. A higher *Precision* ensures the model is less likely to misclassify occupied units to the class of unused. Under the new threshold of 0.7, the number of unused units is reduced to 180,600 from 211,497 in the baseline estimate.

Second, instead of assuming *r* equals 1 when converting LUR to SUR, we consider the possibility that unused units may have a higher probability of being listed on online platforms. Specifically, as described above, the official statistics indicate 85% of housing resales are assisted by professional agents. As a most extreme case, we assume 100% of unused listed units are assisted by agents and therefore appear on online platforms; in this scenario, for each sample city, we can impute the share of occupied units assisted by agents (and hence listed online) based on the estimated LUR, bringing the weighted average of being assisted by agents of both groups to 85%. We then use the imputed *r*, instead of the value of 1, in eq. (5) to convert LUR to SUR.

Carbon emission calculations. *Basic setting*. For city *i*, between 2001 and 2020, we

can observe the annual series of housing completions (in floor area), $AreaCompletion_{i,t}$. Meanwhile, we can impute the annual series of total housing stock (in floor area), $AreaStock_{i,t}$, between 2001 and 2020, which equals

$$AreaStock_{i,t} = AreaStock_{i,t-1} + AreaCompletion_{i,t} - AreaDemolition_{i,t}, \quad (8)$$

where $AreaDemolition_{i,t}$ refers to the floor area of housing demolition in the city-year, which is calculated based on the annual demolition rate of 2% with the expected service lifespan of 50 years as required by the technique code in China[38]. To calculate the housing stock in 2000, we use the city's urban population and per capita living space, as reported by the 2000 Population Census.

Note that, as revealed in this study, a portion of $AreaStock_{i,t}$ had never been occupied by the end of year *t*. Here, we assume the housing stock in 2000 was completely occupied by 2001 due to the inadequate housing supply during the pre-reform era and only consider the unused units completed after 2001. In our data, we can directly observe the SUR associated with each building year cohort in early 2021 (or the end of 2020). Hence, based on $AreaCompletion_{i,t}$ and the building-year-specific SUR, we can calculate the volume of unused housing in each building year cohort at the end of 2020 (SUR of the year 2019 cohort is set as 100% by definition), denoted by $AreaUnused_{i,2020,BuildingYear}$, from $AreaUnused_{i,2020,2001}$ to $AreaUnused_{i,2020,2019}$. Note that, originally, the unused rate is calculated based on the proportion of units, and here we apply it to the floor area volume. Considering that larger units are more likely to be unused, as revealed in Fig. 4 in the main text, this conversion achieves a lower bound of the estimate on unused volume (and the associated carbon emissions). By aggregating the volume of unused housing in the building year cohorts between 2001

and 2019, we can get the total volume of unused housing at the end of 2020, or $AreaUnused_{i,2020}$:

$$AreaUnused_{i,2020} = \sum_{Building\ Year=2001}^{2019} AreaUnused_{i,2020,Building\ Year}. \quad (9)$$

We can then get the floor area of occupied units, or $AreaOccupied_{i,2020}$. Note we assume it is reasonable for any housing unit to be unused during the first two years after its completion, so we also need to further extract the housing completion area in 2020 from the housing stock area in 2020 to calculate the floor area of occupied units at the end of 2020:

$$AreaOccupied_{i,2020} = AreaStock_{i,2020} - AreaUnused_{i,2020} - AreaCompletion_{i,2020}. \quad (10)$$

$AreaOccupied_{i,t}$ can be interpreted as the floor area of actual housing demand in the city-year. For each sample city, we can use the logistic function to regress the annual series of $AreaOccupied_{i,t}$ between 2001 and 2020 and then use the estimated coefficients to forecast $AreaOccupied_{i,t}$ between 2021 and 2030.

Actual carbon emissions in 2020. The residential sector's overall carbon emissions consist of the construction and operation stages. The volume of residential building construction emissions in year t, $CE\_C\_Actual_{i,t}$, is calculated as follows:

$$CE\_C\_Actual_{i,t} = AreaCompletion_{i,t} * CO2\_C_{i,t}, \quad (11)$$

where $CO2\_C_{i,t}$ refers to the embodied carbon intensity factor during the construction stage (including the construction material productions, such as cement and steel) for the residential sector in year t.

For the operation stage, the volume of carbon emissions of the residential building stock in year t, $CE\_O\_Actual_{i,t}$, is calculated as

$$CE\_O\_Actual_{i,t} = AreaOccupied_{i,t} * (CO2\_O_{i,t} + CO2\_CH_{i,t}) + AreaUnused_{i,t} * CentralHeating_i * CO2\_CH_{i,t}, \quad (12)$$

where $CO2\_O_{i,t}$ indicates the operational carbon intensity factor (such as cooking and lighting) in China's residential sector, and for cities located in Northern China, we also consider the carbon emissions associated with residential heating, with the intensity factor of $CO2\_CH_{i,t}$. Here, we assume an unused unit does not generate operational carbon emissions. As for the heating emissions, we assume that if an unused unit uses the individual household based heating system, the owner will turn off the system, and hence, the unit would no longer generate heating emissions. However, for dwelling buildings with central-heating systems, whose proportion in Northern Chinese cities reaches as high as 90% according to our dataset, the heating systems still work for the unused dwelling units. For this purpose, we adopt $CentralHeating_i$ to indicate the proportion of unused housing with central heating in city i, which is calculated based on the same dataset of listing-unit information that we use to calculate LUR.

The three carbon intensity factors ($CO2\_C_{i,t}$, $CO2\_O_{i,t}$, and $CO2\_CH_{i,t}$) indicate China's decarbonization efforts in the residential sector. Specifically, we consider four key decarbonization measures: lowering steel- and cement-production carbon intensity and promoting prefabricated buildings, which can lower $CO2\_C_{i,t}$, and promoting green buildings and renovating existing buildings for energy efficiency improvement, which can lower $CO2\_O_{i,t}$ and $CO2\_CH_{i,t}$. Specifically, we adopt 465.59 kg/m^2 for $CO2\_C_{i,2000}$, 40.76 kg/m^2 for $CO2\_O_{i,2000}$, and 30.86 kg/m^2 for $CO2\_CH_{i,2000}$[22-25,39-42]. Then, based on the official reports on the progress of these four measures, the quantitative estimate of their effect on carbon emission intensity found in the literature[22-25,43-46], and the composition of the housing stock, we calculate the carbon

intensity factors for each subsequent year.

Finally, we can have the city-level total emission volume in any specific year. Take the year 2020 as an example:

$$CE\_Actual_{i,2020} = CE\_C\_Actual_{i,2020} + CE\_O\_Actual_{i,2020}. \quad (13)$$

Carbon emissions from unused housing in 2020. For each square meter of dwelling space that remained unused at the end of 2020 (note we do not include the carbon emissions of unused units completed in 2019 and 2020, because we assume they are not preventable), we consider its related carbon emissions from two perspectives. The carbon emissions for the operation stage are straightforward: as described in the previous subsection, we assume unused housing does not generate operational carbon emissions, but it would still incur central-heating emissions if it is located in a northern city. For the construction stage, we convert the lump-sum construction emissions to the annual amortized emissions[47]. Because the literature has not achieved a consensus on the "discount rate" of carbon emissions, we choose to evenly amortize the construction carbon emissions on the expected service lifespan of 50 years. Because, by definition, the unused period can only exist at the beginning of the lifespan, adopting the 0% discount rate (i.e., even amortization) achieves a lower bound of the annual amortized emissions. Therefore, for dwelling units that were completed in the year *BuildingYear* and remained unused at the end of 2020, the associated waste in carbon emissions in 2020 can be calculated as

$$\begin{aligned} CE\_Unused_{i,2020} = \sum_{BuildingYear=2001}^{2018} CE\_Unused_{i,2020,BuildingYear} = \\ \sum_{BuildingYear=2001}^{2018} (2\% * AreaUnused_{i,2020,BuildingYear} * CO2\_C_{i,BuildingYear} + \\ AreaUnused_{i,2020,BuildingYear} * CentralHeating_i * CO2\_CH_{i,2020}). \end{aligned} \quad (14)$$

Carbon emission reductions by decarbonization measures in 2020. We consider a

scenario in which none of the four decarbonization initiatives are implemented and the carbon intensity factors remain constant at 2000 levels. In this non-decarbonization scenario, the residential sector's total carbon emissions can be calculated as

$$CE\_High_{i,2020} = AreaCompletion_{i,2020} * CO2\_C_{i,2000} + AreaOccupied_{i,2020} * (CO2\_O_{i,2000} + CO2\_CH_{i,2000}) + AreaUnused_{i,2020} * CentralHeating_i * CO2\_CH_{i,2000}. \quad (15)$$

The difference between $CE\_High_{i,2020}$ and $CE\_Actual_{i,2020}$ reflects the carbon-emission-reduction contribution of these four decarbonization measures.

Forecast on carbon emissions in 2021–2030. Based on $AreaOccupied_{i,t}$, we can impute the series of annual floor areas of housing completion between 2021 and 2030, $AreaCompletion\_Base_{i,t}$, which could make the unused rate remain at the same level as the end of 2020. Specifically, recall the SUR is defined as

$$UnusedRate_{i,t} = UnusedRate_{i,2020} = (AreaStock_{i,t} - AreaOccupied_{i,t})/AreaStock_{i,t}. \quad (16)$$

Based on eq. (8) and eq. (16), we can have

$$AreaCompletion\_Base_{i,t} = \{(AreaStock_{i,t-1} - AreaDemolition_{i,t}) * (UnusedRate_{i,2020} - 1) + AreaOccupied_{i,t}\}/(1 - UnusedRate_{i,2020}). \quad (17)$$

We also assume the carbon intensity factors are consistent with those in 2020. Based on these assumptions, the carbon emission in the baseline scenario equals

$$CE\_Baseline_i = \sum_{t=2021}^{2030} \left(AreaCompletion_{Base_{i,t}} * (CO2\_C_{i,2020} + AreaOccupied_{i,t} * (CO2\_C_{i,2020} + CO2\_CH_{i,2020}) + (AreaStock_{i,t} - AreaOccupied_{i,t}) * CentralHeating_i * CO2\_CH_{i,2020}\right). \quad (18)$$

In the following scenarios, we assume the unused rate of each city at the end of 2030 gradually reduces to 75%, 50%, and 25% of the level observed at the end of 2020.

Utilizing these assumed rates of unused housing, we can impute the series of annual floor areas of housing completion by using the corresponding $UnusedRate_{i,t}$ in eq. (17), as well as the annual series of $AreaStock_{i,t}$. We can then calculate the total carbon emissions in 2021–2030 in the city under each scenario.

Data availability

All macro-level data necessary for replication will be available at the public repository to reproduce the results presented in this paper upon publication.

Code availability

All code necessary for replication will be available at the public repository to reproduce the results presented in this paper upon publi cation.

References

26. Liu, X.-Y., Wu, J. & Zhou, Z.-H. Exploratory undersampling for class-imbalance learning. *IEEE Trans. Syst. Man Cybern. Part B-Cybern.* **39**, 539-550 (2008).
27. Chawla, N. V., Japkowicz, N. & Kotcz, A. Special issue on learning from imbalanced data sets. *SIGKDD Explor. Newsl.* **6**, 1-6 (2004).
28. Jung, H. et al. ResNet-Based Vehicle Classification and Localization in Traffic Surveillance Systems. In *Proc. IEEE Conference on Computer Vision and Pattern Recognition Workshops (CVPRW)* 934-940 (IEEE, 2017); https://doi.org/10.1109/CVPRW.2017.129
29. Rezende, E., Ruppert, G., Carvalho, T., Ramos, F. & de Geus, P. Malicious Software Classification Using Transfer Learning of ResNet-50 Deep Neural Network. In *Proc. IEEE International Conference on Machine Learning and Applications (ICMLA)* 1011-1014 (IEEE, 2017); https://doi.org/10.1109/ICMLA.2017.00-19
30. Habibzadeh Motlagh, M., Jannesari, M., Rezaei, Z., Totonchi, M. & Baharvand, H. Automatic white blood cell classification using pre-trained deep learning models: ResNet and Inception. In *Proc. International Conference on Machine Vision (ICMV)* (eds. Zhou, J., Radeva, P., Nikolaev, D. & Verikas, A.) 105 (SPIE, 2018); https://doi.org/10.1117/12.2311282
31. He, K., Zhang, X., Ren, S. & Sun, J. Deep Residual Learning for Image Recognition. In *Proc. IEEE Conference on Computer Vision and Pattern Recognition (CVPR)* 770-778 (IEEE, 2016); https://doi.org/10.1109/CVPR.2016.90
32. Krizhevsky, A., Sutskever, I. & Hinton, G. E. Imagenet classification with deep

convolutional neural networks. *Commun. ACM* **60**, 84-90 (2017).
33. Lewis, D. D., Yang, Y., Russell-Rose, T. & Li, F. RCV1: A new benchmark collection for text categorization research. *J. Mach. Learn. Res.* **5**, 361-397 (2004).
34. Pillai, I., Fumera, G. & Roli, F. Designing multi-label classifiers that maximize F measures: State of the art. *Pattern Recognit.* **61**, 394-404 (2017).
35. Davis, J. & Goadrich, M. The relationship between Precision-Recall and ROC curves. In *Proc. International Conference on Machine Learning (ICML)* 233-240 (ACM Press, 2006); https://doi.org/10.1145/1143844.1143874
36. Han, L. & Strange, W. C. *Handbook of regional and urban economics* Vol. 5 (eds Gilles Duranton, Vernon Henderson, & William Strange) 813-886 (North-Holland, 2015).
37. Zheng, S., Liu, H. & Lee, R. Buyer search and the role of broker in an emerging housing market: a case study of Guangzhou. *Tsinghua Sci. Technol.* **11**, 675-685 (2006).
38. Ministry of Housing and Urban-Rural Development. *Unified Standard for Reliability Design of Building Structures GB 50068-2018* (China Architecture & Building Press, 2018).
39. Yang, D. et al. Urban buildings material intensity in China from 1949 to 2015. *Resour. Conserv. Recycl.* **159**, 104824 (2020).
40. Chen, W., Yang, S., Zhang, X., Jordan, N. D. & Huang, J. Embodied energy and carbon emissions of building materials in China. *Build. Environ.* **207**, 108434 (2022).
41. Zhang, Y., Yan, D., Hu, S. & Guo, S. Modelling of energy consumption and carbon emission from the building construction sector in China, a process-based LCA approach. *Energy Policy* **134**, 110949 (2019).
42. Jiang, J. China's urban residential carbon emission and energy efficiency policy. *Energy* **109**, 866-875 (2016).
43. Hao, J. et al. Carbon emission reduction in prefabrication construction during materialization stage: A BIM-based life-cycle assessment approach. *Sci. Total Environ.* **723**, 137870 (2020).
44. Teng, Y., Li, K., Pan, W. & Ng, T. Reducing building life cycle carbon emissions through prefabrication: Evidence from and gaps in empirical studies. *Build. Environ.* **132**, 125-136 (2018).
45. Wu, X., Peng, B. & Lin, B. A dynamic life cycle carbon emission assessment on green and non-green buildings in China. *Energy Build.* **149**, 272-281 (2017).
46. Li, J. & Shui, B. A comprehensive analysis of building energy efficiency policies in China: status quo and development perspective. *J. Clean Prod.* **90**, 326-344 (2015).
47. Maciel, V. G. et al. Towards a non-ambiguous view of the amortization period for quantifying direct land-use change in LCA. *Int. J. Life Cycle Assess.* **27**, 1299-1315 (2022).

Acknowledgments

We highly appreciate Joseph Gyourko, Yu Qin, Xiaodong Li, and Chen Zhu for their valuable comments. Linzhen Zhu provides outstanding research assistance. We are also

grateful for the funding by the National Natural Science Foundation of China (Project No: 72174100, 71874093).

Author Contributions

Wu J. and Zhang R. raised the research idea. Zheng H. and Wu J. collected data. Zheng H. and Zhang R. designed and trained the deep learning model. Yin X. and Zheng H. calculated the carbon emissions. All the authors wrote the manuscript.

Competing Interests

The authors declare no competing interests.

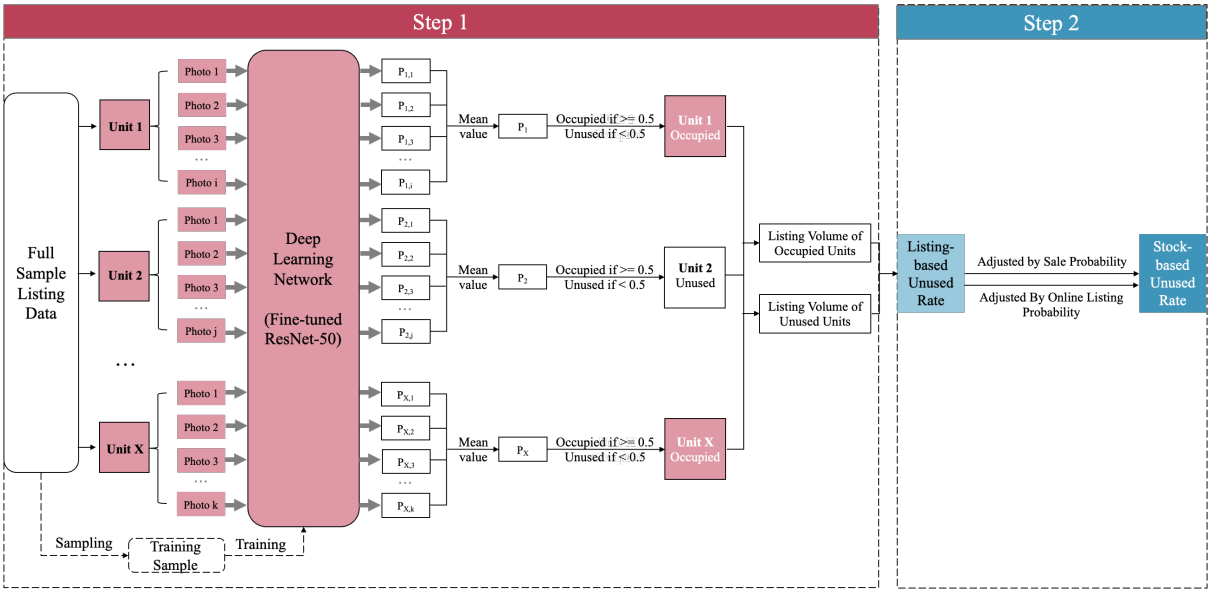

Fig. 1 | Method of Estimating Unused Housing Rate. This figure displays our conceptual method of calculating the stock-based unused housing rate based on the listing dataset. Step 1 presents the method of identifying all the unused dwelling units for each sample city using a supervised deep learning network, whose details are shown in Extended Data Fig. 6. See Extended Data Fig. 1 for examples of photo-level classifications about the use status. Step 2 converts the listing-based unused rate into the stock-based unused rate.

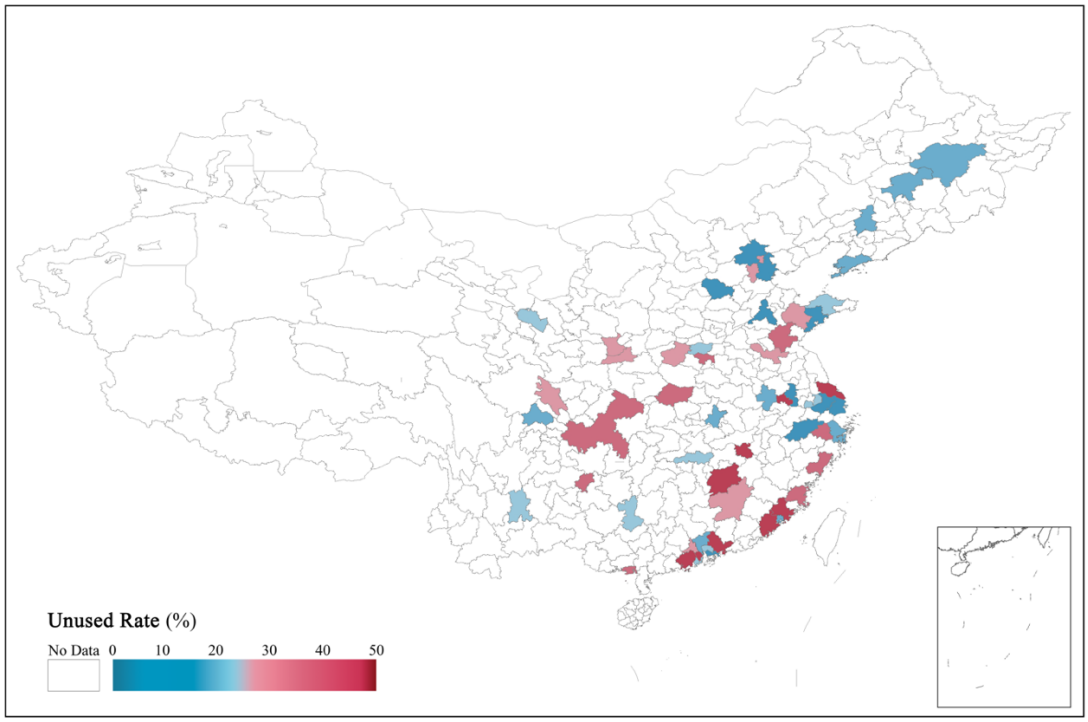

Fig. 2 | City-Level Unused Housing Rates in the Baseline Scenario. This map displays the spatial distribution of city-level SURs in the baseline scenario in early 2021. The unused rate for each city is denoted by the gradient from dark blue to dark red. Red denotes cities where the SURs are higher than the median, whereas blue denotes cities lower than the median. Blank spaces indicate data unavailability. Extended Data Fig. 2 reproduces this figure under a conservative scenario. The base map is from the website of the Ministry of Natural Resources, China.

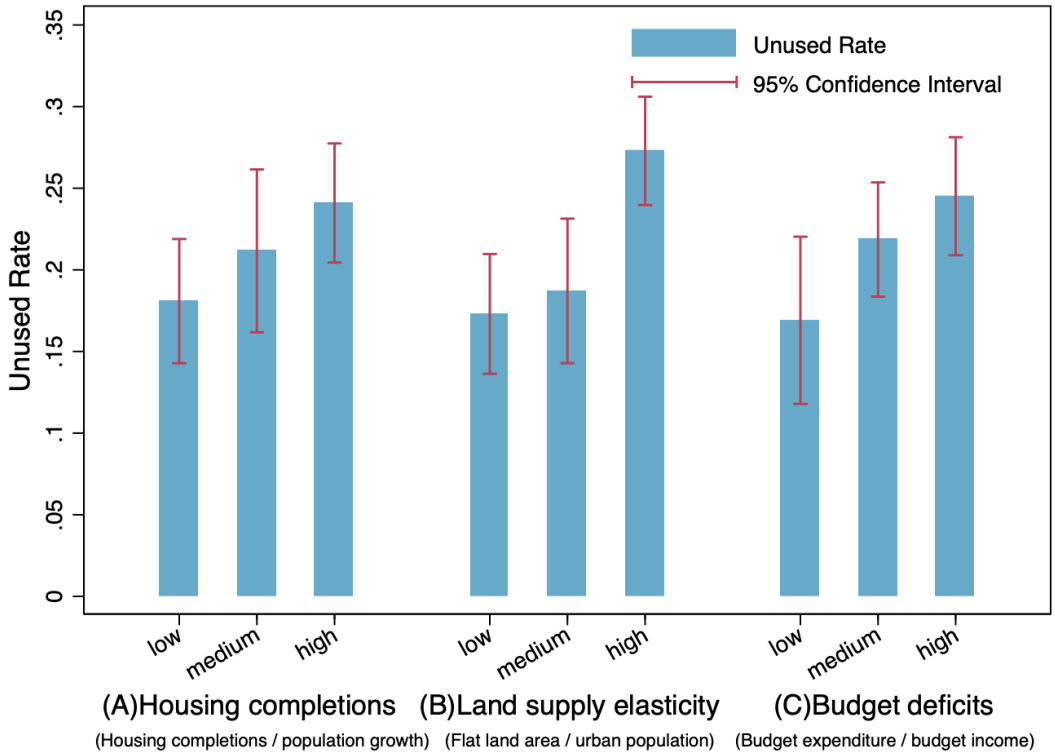

Fig. 3 | Relationship between Housing Oversupply and Unused Rates. The blue bars indicate the mean value of city-level SURs for the low, medium, and high groups, divided based on the tertiles in terms of **(A)** the ratio between aggregated housing completions in 2001–2020 and population growth during the same period, which indicates excess housing supply, **(B)** the quantity of flat land area in the city normalized by the population in 2000, which measures the land supply elasticity, and **(C)** the government budget deficits in 2001–2020, which measures local governments' incentives to sell residential land. Error bars depict 95% confidence intervals.

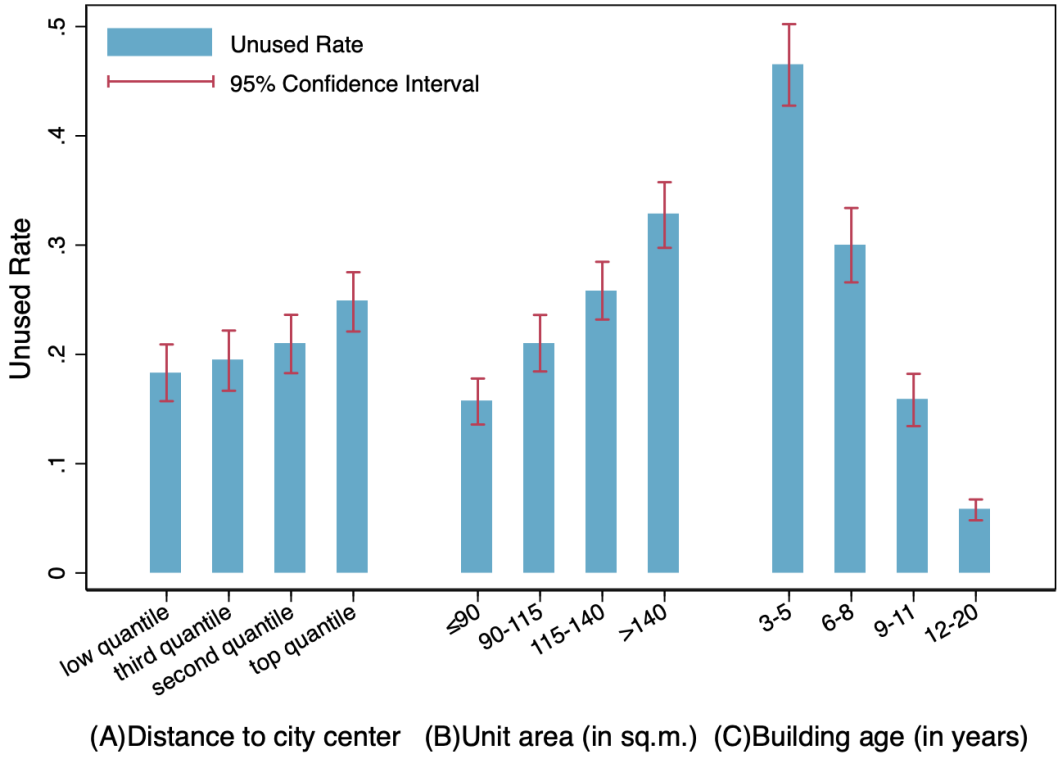

Fig. 4 | Within-City Variances of the Unused Rate. (A) indicates the mean value of the community-level SURs for the four groups, divided based on the quantiles of distance to the city center, respectively. **(B)** indicates the mean value of the unit-level SURs for the groups with unit areas of no more than 90 sq.m, between 90 and 115 sq.m, between 115 and 140 sq.m, and more than 140 sq.m, respectively. **(C)** indicates the mean value of the unit-level SURs for the groups with building years between 3 and 5 years, 6–8 years, 9–11 years, and 12–20 years, respectively. Error bars depict 95% confidence intervals.

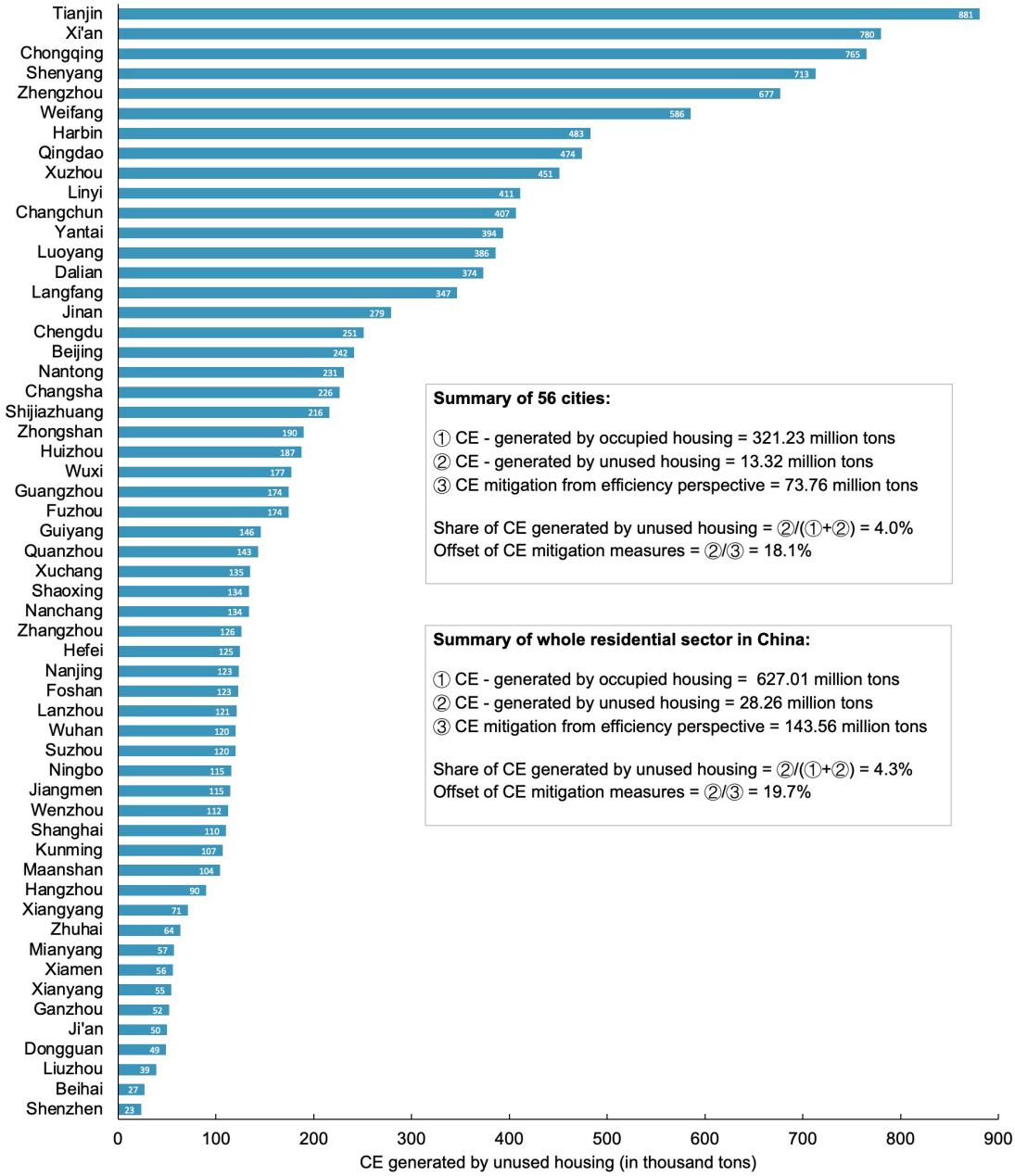

Fig. 5 | Impact of Unused Housing on Carbon Emissions in 2020. This figure depicts the city-level carbon emissions generated by unused housing in 2020. The 56 cities in our sample are sorted by the total carbon emissions generated by unused housing in 2020.

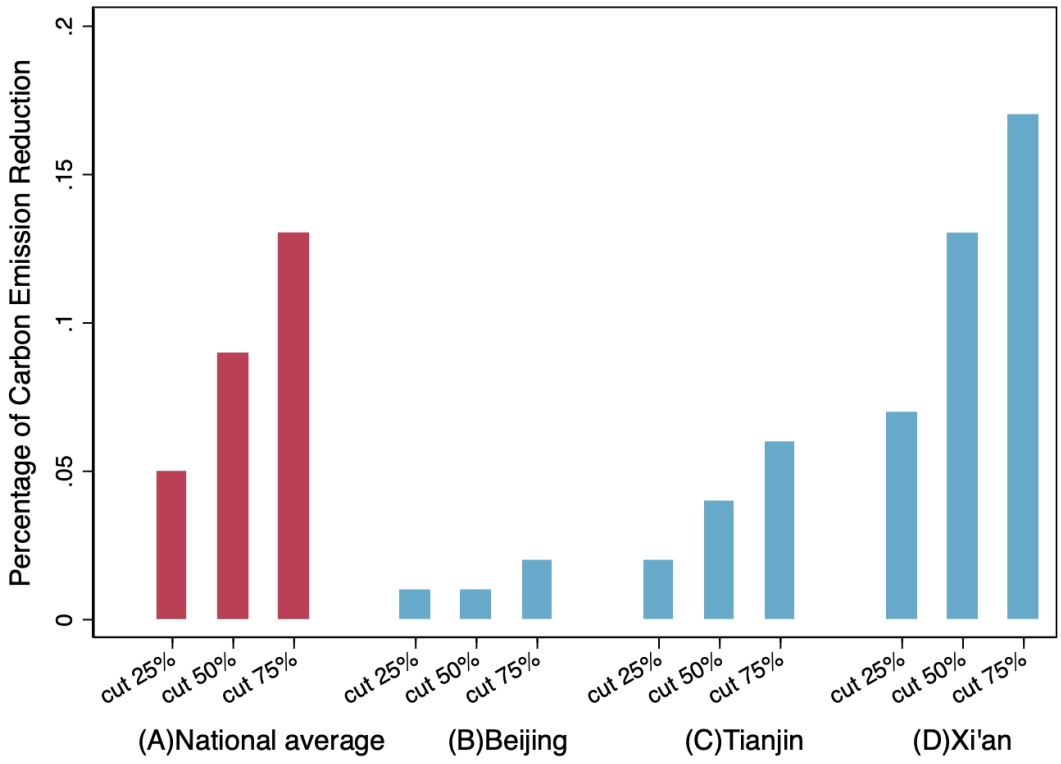

Fig. 6 | Contribution of Unused Rate Decreasing on Carbon Emission Reductions in 2021-2030. This figure indicates the percentage of carbon emission reduction in Chinese residential sector after the unused rate is gradually cut off by 25%, 50%, and 75% throughout 2021 and 2030, respectively. The benchmark scenario is that the unused rate at the end of 2030 remains at the same level as at the end of 2020 (for the national average, we adopt the weighted average of 56 sample cities). We make a forecast from both the national level **(A)** and for three representative cities: **(B)** Beijing, which represents the cities with low unused rates; **(C)** Tianjin, which represents the cities with medium unused rates; and **(D)** Xi'an, which represents the cities with high unused rates.

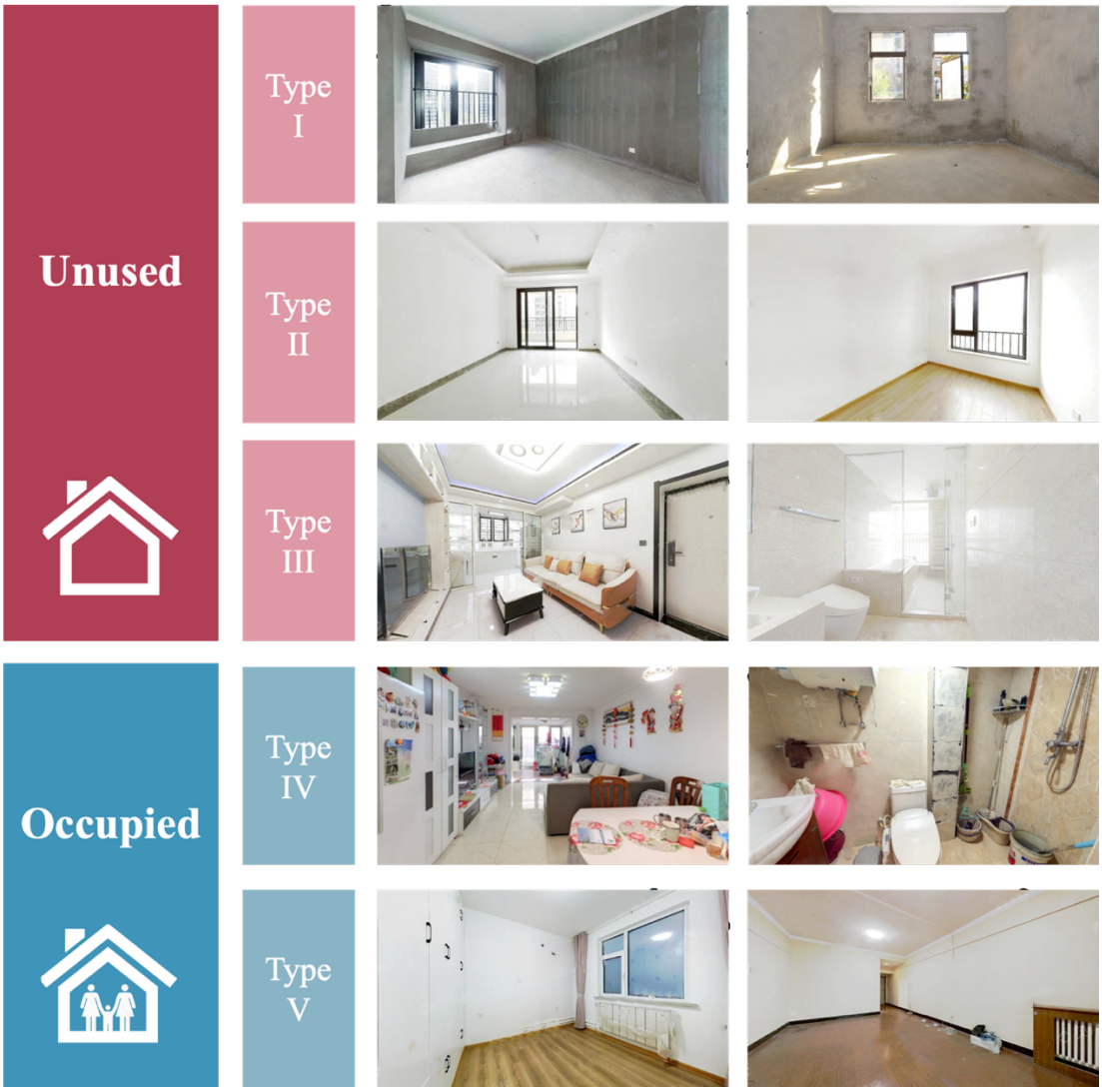

Extended Data Fig. 1 | Examples of Photos for Unused and Occupied Dwelling Units. This figure displays representative examples of indoor photos from the online housing listing platform. The rooms in Type I belong to units without interior decoration, whereas the rooms in Type II are partially decorated; obviously, neither of these two types of units meets the ordinary living standard. The Type III rooms are well decorated, but their pristine state and brand-new furniture indicate they have never been inhabited. Type IV rooms, on the other hand, are filled with an abundance of daily items, showing they are currently occupied. Type V rooms are nearly empty; nevertheless, we can still infer that the rooms were once occupied based on the traces of usage on the walls, floors, and ceilings, even if the owners/renters have moved out. Accordingly, we classify the dwelling units in Types I, II, and III as "unused," and units in Types IV and V as "occupied."

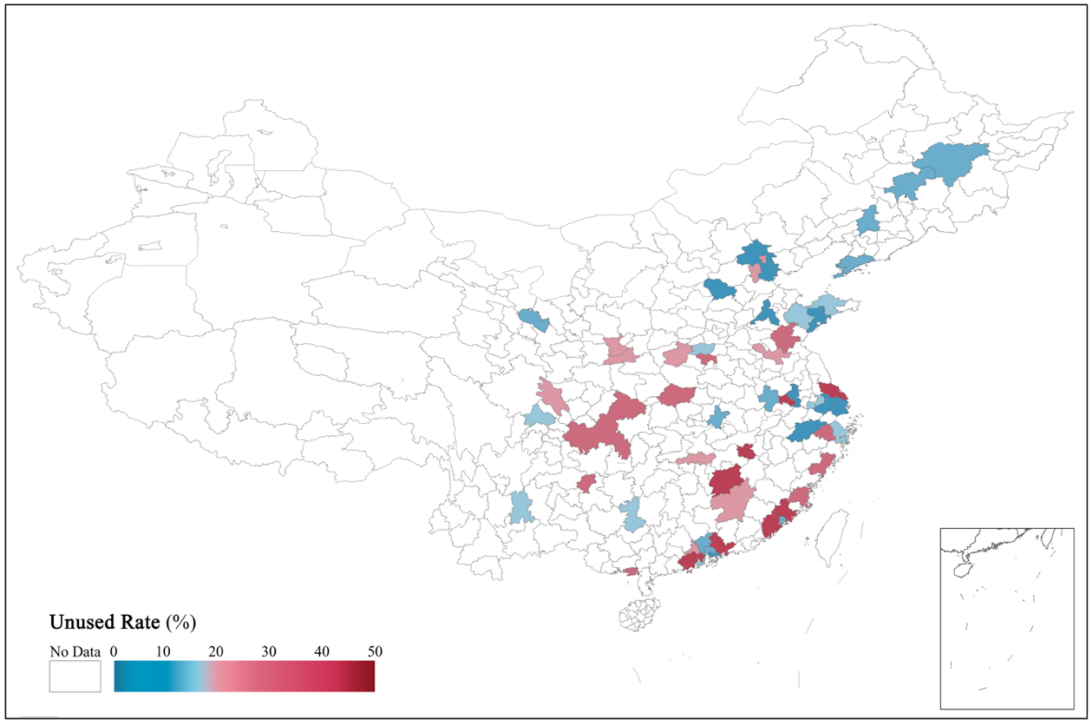

Extended Data Fig. 2 | City-Level Unused Housing Rates in the Conservative Scenario. This map displays the spatial distribution of city-level SURs in the conservative scenario, which is reproduced based on Fig. 2.

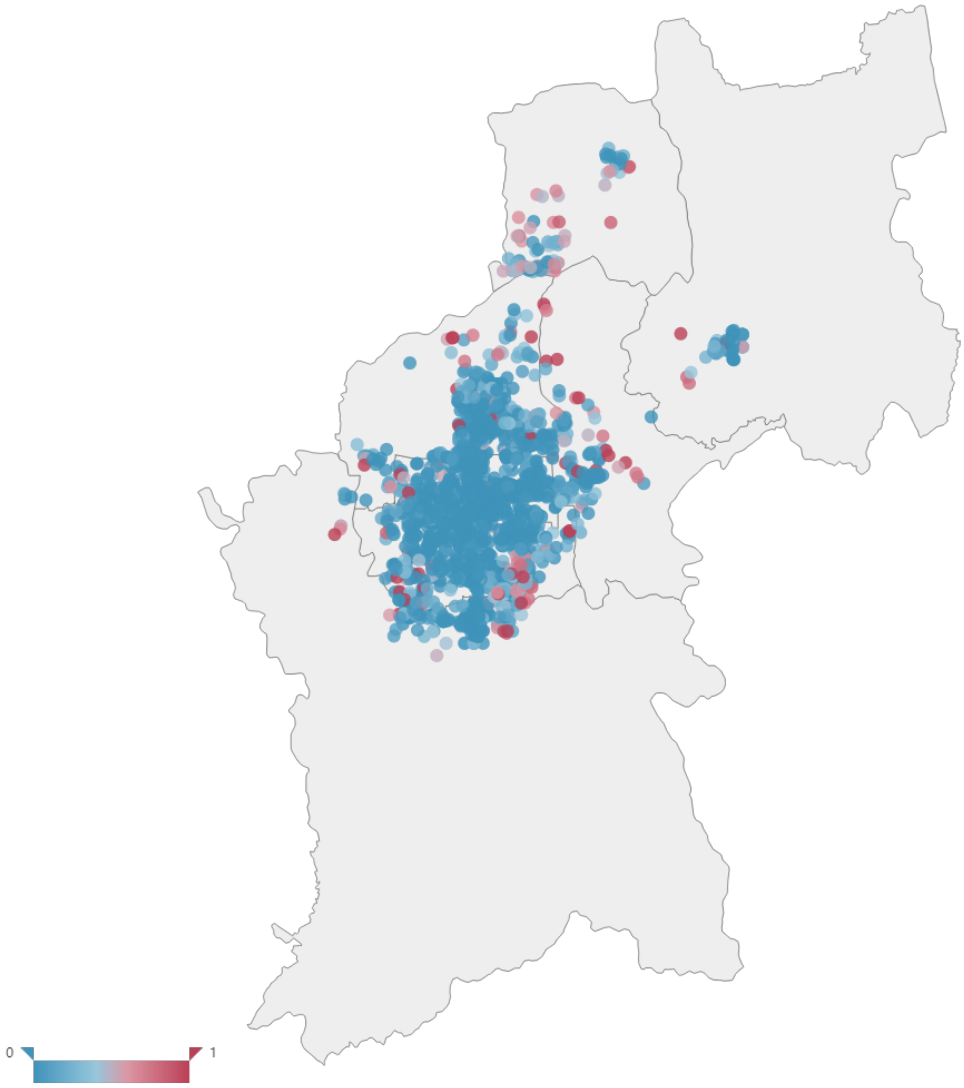

Extended Data Fig. 3 | Community-Level Unused Housing Rates in Xi'an. This map displays the spatial distribution of communities in Xi'an. The LUR for each community is denoted by the gradient from dark blue to dark red.

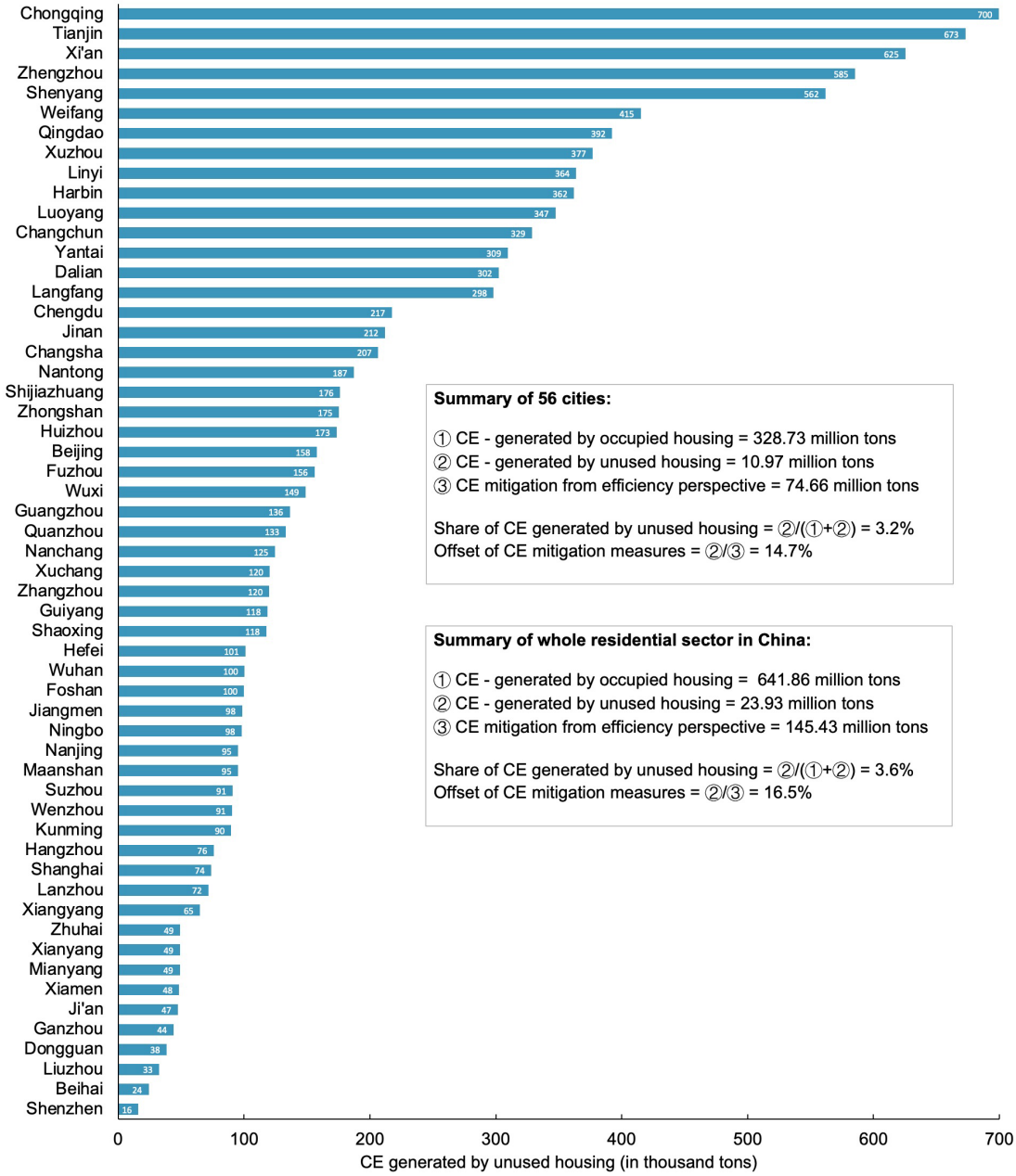

Extended Data Fig. 4 | Impact of Unused Housing on Carbon Emissions in 2020. This figure depicts the city-level carbon emissions generated by unused housing in 2020 in the conservative scenario, which is reproduced based on Fig. 5.

Extended Data Fig. 5 | Example of Online Housing Listing Webpage. This figure provides a representative example of an online housing listing webpage on the platform from which we collected the listing information. As required by the platform, we omit all information that can be used to trace the agent's or platform's name.

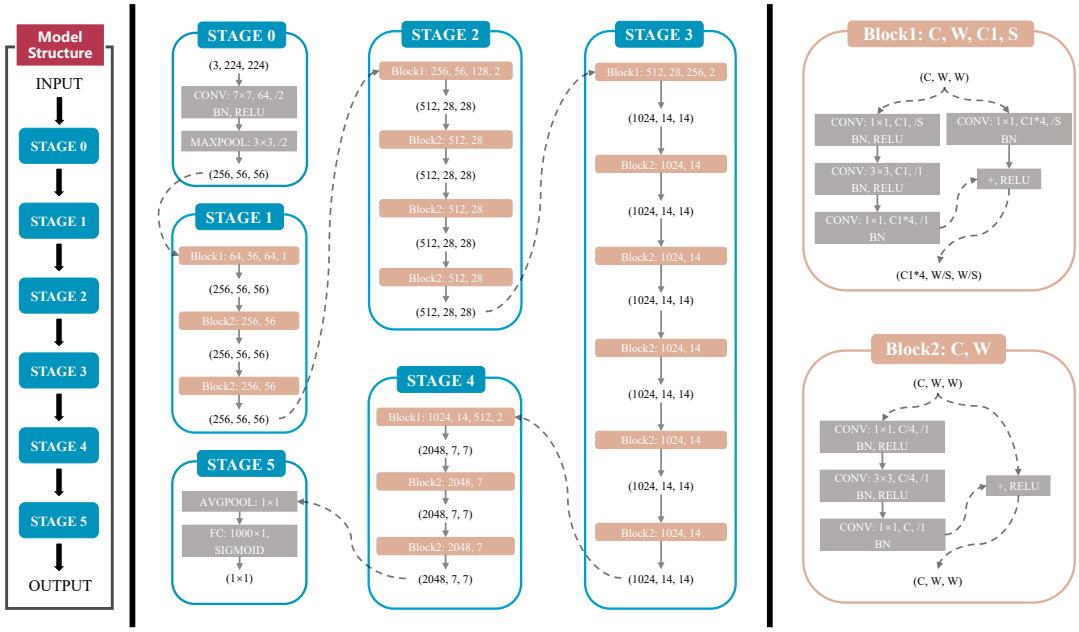

Extended Data Fig. 6 | Architecture of the Classification Network. This graph illustrates the detailed architecture of the deep learning network depicted in Step 1 of Fig. 1.

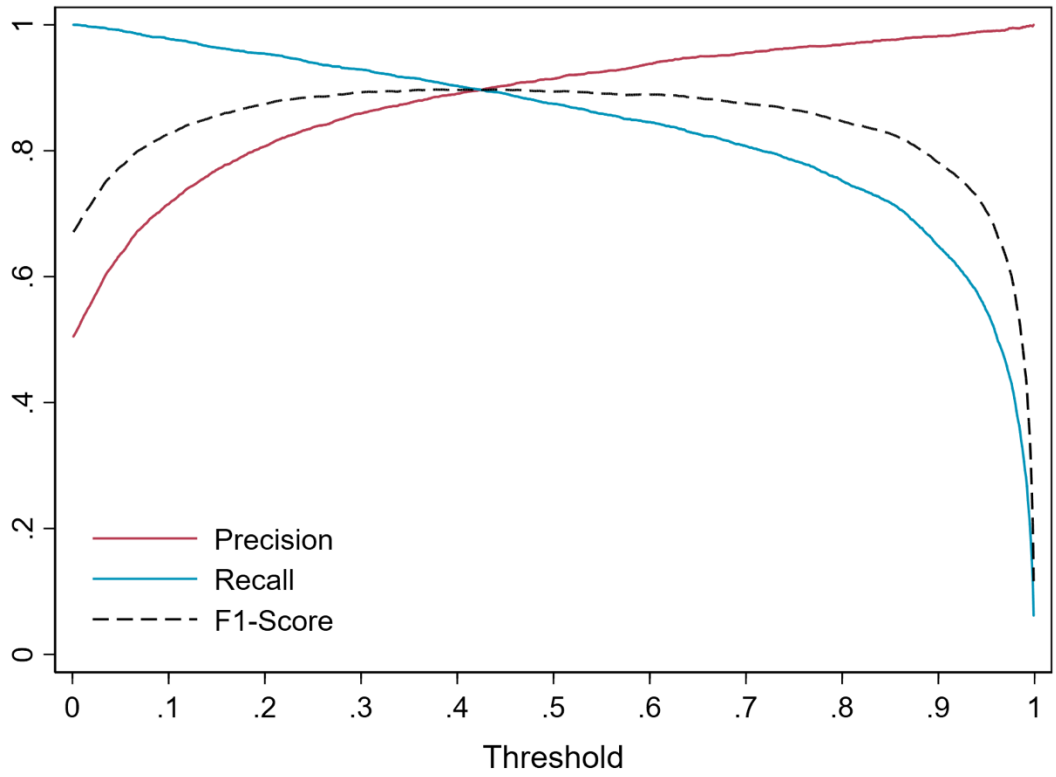

Extended Data Fig. 7 | Relationship between F1-Score and Threshold at the Photo-Level Classification. This graph depicts the three metrics of the training outcome of the classification model under various thresholds. The red line denotes the metric of precision, which reflects the ability of a classification model to identify only relevant data. The blue line denotes the metric of recall, which reflects the ability to identify all relevant cases within a dataset. The dashed line denotes the F1-Score (i.e., the harmonic mean of "Precision" and "Recall"), by which we can comprehensively assess the performance of the model.

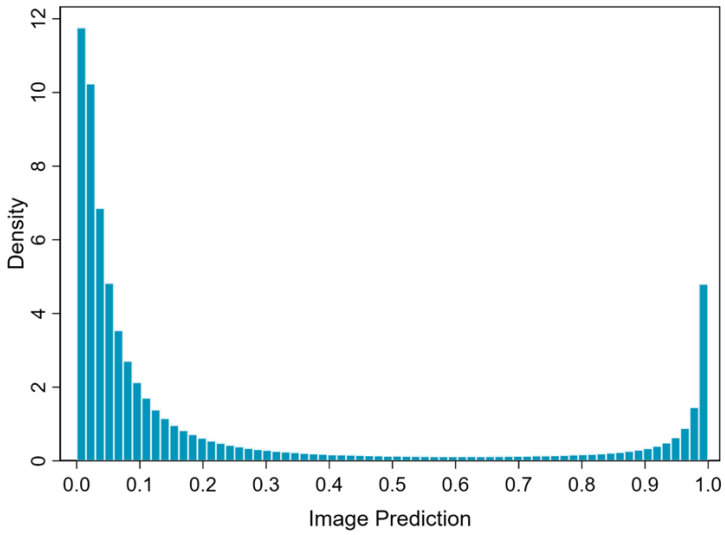

(A) Photo Level

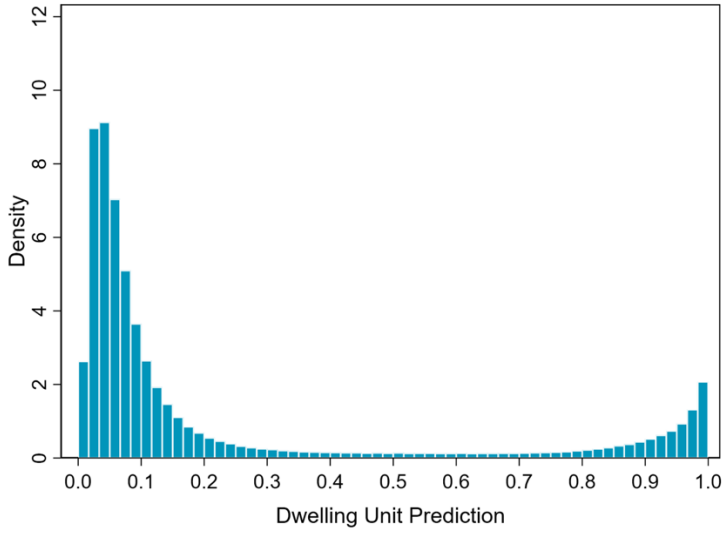

(B) Unit Level

Extended Data Fig. 8 | Distribution of Classification Results. (A) depicts the distribution of the prediction results of the classification model at the photo level, which refers to the probability of being unused, $P_{x,k}$, in Step 1 of Fig.1. **(B)** depicts the distribution of prediction results of the classification model at the unit level, which refers to the probability of being unused, P_x, in Step 1 of Fig.1.

Extended Data Table 1: Tag Distribution in the Training Sample

	Original (Before Undersampling)	Working (After Undersampling)
Unused	38,322	38,322
Occupied	195,574	38,322

This table reports the tag results for photos in the training sample before and after undersampling.

Extended Data Table 2: Differences in LUR Based on Two Online Platforms

City	LUR Based on Our Platform	LUR Based on Another Leading Platform	LUR Difference
A	2.91%	3.33%	-0.42%
B	8.68%	7.47%	1.21%
C	12.35%	11.69%	0.66%
D	20.83%	22.89%	-2.06%
E	40.95%	38.46%	2.49%

This table reports the city-level LURs calculated based on the listing data for five sample cities between November 2020 and March 2021 from both our online platform and another leading online listing platform in China.